Gate-Controlled Superconducting Proximity Effect in Carbon Nanotubes

A. F. Morpurgo,[1]* J. Kong,[2] C. M. Marcus,[1]* H. Dai[2]

The superconducting proximity effect in single-walled carbon nanotubes connected to niobium electrodes was controlled with the use of nearby gates that tune the niobium-nanotube transparency. At 4.2 kelvin, when the transparency was tuned to be high, a dip in the low-bias differential resistance was observed, indicating a proximity effect mediated by Andreev reflection. When the transparency was tuned to be low, signatures of Andreev reflection disappeared and only tunneling conduction was observed. Below ~4 kelvin, a narrow peak in differential resistance around zero bias appeared superimposed on the Andreev dip, probably as a result of electron-electron interaction competing with the proximity effect.

The electronic properties of a normal conductor are modified by the presence of a nearby superconductor, a phenomenon known as the superconducting proximity effect. This effect has been widely investigated for two- and three-dimensional metallic and semiconducting structures and is now well understood (*1*). The situation is different for strictly one-dimensional (1D) systems, where intrinsic electronic properties are expected to differ qualitatively from those in higher dimensions (*2*) and experimental work is hampered by the difficulty of fabricating and probing 1D structures. The discovery of single-walled carbon nanotubes (SWNTs) (*3*), long cylindrical carbon molecules with diameters in the nanometer range, has changed the experimental situation. These molecules constitute an experimentally accessible model system of a 1D electron liquid (*4*–*10*) and offer new opportunities to control transport properties, in 1D conductors. Here, we show that the superconducting proximity effect in SWNTs (*10*) can be controlled by means of a gate voltage.

The experimental system we consider consists of SWNTs between two superconducting Nb electrodes fabricated on a Si substrate. Fabrication of the nanotubes is based on chemical vapor deposition (CVD) using flowing methane gas and a catalyst to seed the growth of individual SWNTs (*11*). Pairs of 5 μm by 5 μm islands of catalyst with separations ranging from 0.3 to 3 μm are patterned on a thermally oxidized Si wafer by means of electron-beam lithography and lift-off techniques. The CVD process frequently yields one or more SWNTs connecting pairs of islands. In a second lithographic step, 60 nm of Nb covered by 20 nm of Au is sputtered on top of the catalyst in patterned regions that extend over the sides of the islands, providing direct electrical contact between the Nb and the SWNTs. In a final processing step, the Nb electrodes are connected to large Ti-Au bonding pads. Not all SWNTs conduct at low temperature, nor do all contacts have low resistance; hence, pad spacing is optimized to yield typically three or four individual SWNTs interconnecting the electrodes (Fig. 1), leading to a large number of samples whose electrical characteristics are suitable for the present investigation.

Low-temperature transport measurements of current I and of differential resistance, dV/dI, versus bias voltage V are made in a two-lead configuration with a series resistance of ~20 ohms, a negligible value relative to the resistance of the sample. The Si substrate is highly doped and remains conducting at low temperature, so that it can be used as a back gate (*12*) separated from the SWNTs by a 0.5-μm layer of insulating SiO_2. Data from five samples with Nb pads separated by 0.3 μm are reported. All samples exhibit the same qualitative behavior.

Typical *I-V* measurements at 4.2 K for gate voltages $V_g = 0$ V and -40 V (Fig. 2) demonstrate that a large negative gate voltage decreases the overall sample resistance. From the change in total sample resistance alone, one cannot conclude whether the gate voltage acts to change the resistance of the metallic SWNTs themselves or the transparency of the contacts. However, changes in the shape of dV/dI with gate voltage in the presence of superconducting leads indicate that it is predominantly the contact transparency that changes, as described below. This conclusion is consistent with observations that the typical resistance among a batch of samples does not depend on the length of the SWNTs, and hence it is the contacts that dominate the total resistance (*13*).

The important feature of the *I-V* curves of samples with superconducting contacts is a change in nonlinearity with gate voltage (Fig. 2). For $V_g = 0$, the slope of the *I-V* curve, dV/dI, has a maximum around zero bias, whereas for $V_g = -40$ V, dV/dI has a minimum around zero bias. This behavior is clearly seen in the dV/dI measurements of the samples with super-

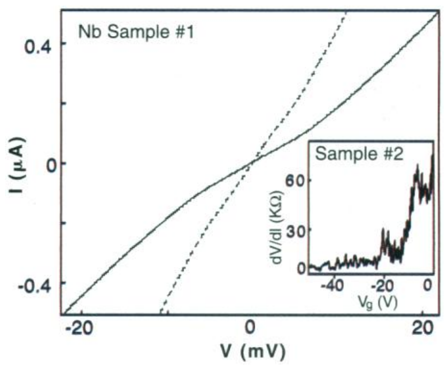

Fig. 2. *I-V* curves measured at $V_g = 0$ V (solid line) and $V_g = -40$ V (dashed line) ($T = 4.2$ K). The gate voltage affects both the resistance and the nonlinearity of the *I-V* curve. Inset: Typical gate voltage dependence of the zero-bias resistance. For all samples the resistance is lowered at 4.2 K by applying a large negative gate voltage.

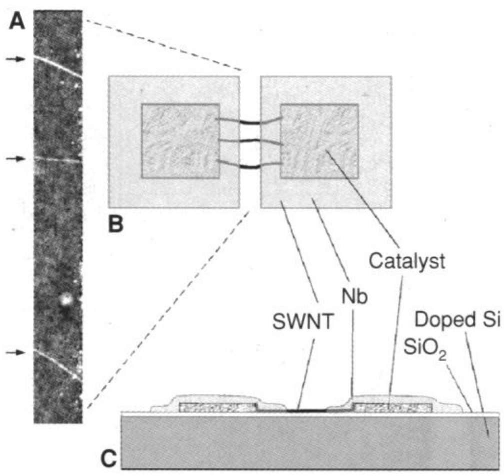

Fig. 1. Schematic of sample layout, showing SWNTs grown from two 5 μm by 5 μm catalyst islands, then covered with 600 Å of sputtered Nb, producing a 300-nm gap between Nb pads. (**A**) Atomic force microscope image of gap region between Nb pads, with three SWNTs (marked with arrows) visible. (**B** and **C**) Top and side views of schematic device layout. Atomic force microscope images show that the diameters of all SWNTs are <1.6 nm (except for one SWNT in one of the five samples measured, which has a diameter of 1.8 nm).

[1]Department of Physics, [2]Department of Chemistry, Stanford University, Stanford, CA 94305, USA.

*To whom correspondence should be addressed. E-mail: morpurg1@leland.stanford.edu, cmarcus@stanford.edu

conducting leads (Fig. 3, A and B), and differs markedly from that of SWNTs with normal metal (Ti-Au) contacts (Fig. 3C). Samples with normal metal contacts show only a broad, featureless peak in *dV/dI* around zero bias, which increases in amplitude as the temperature is lowered and which is larger for samples with higher resistance. The effect of V_g in samples with normal metal contacts is to change the overall resistance of the sample, but not the shape of *dV/dI* versus *V*.

The strong, gate voltage–dependent features in *dV/dI* for the case of superconducting contacts appear at bias voltages of ~2 to 3 meV, close to twice the superconducting gap of Nb ($2\Delta_{Nb} \sim 2.9$ meV), as expected for two Nb-SWNT junctions connected in series (*14*). These features appear superimposed on a broad nonlinear background similar to what is seen for normal metal contacts. At temperatures above the critical temperature T_c of Nb (~9.2 K), the gate voltage–dependent features disappear but the background remains essentially unchanged (Fig. 4).

These observations indicate that the features in *dV/dI* that are strongly dependent on gate voltage result from the presence of the superconducting electrodes, whereas the broad background peak does not. This broad peak is presumably due to electron-electron interaction effects in the SWNTs, and, as shown by Bockrath *et al.* (*8*), has properties that are consistent with a Luttinger liquid model of SWNTs. These coexisting features suggest that electron-electron interactions compete with proximity effects in this system.

Despite these possibly important electron-electron interaction effects, one may gain at least a qualitative understanding of the superconductivity-related phenomena observed at 4.2 K from a noninteracting picture of electron transport in a SWNT. Without interactions, transport across a single superconducting normal interface can be described in terms of a competition between normal and Andreev scattering processes, depending on the transparency of the interface (*15*). Within this theory, at high interface transparency the Andreev reflection process—in which an incident electron is converted into a Cooper pair, leaving a reflected hole in the normal region (*16*)—occurs with large probability, leading to a reduction in the resistance below the superconducting gap. At low interface transparency—the so-called tunneling regime—Andreev reflection occurs with small probability and a peak in differential resistance is found at biases below the gap. For our experimental system, which contains two SWNT-Nb interfaces, a complete model should in principle take into account multiple Andreev reflections that would give rise to subharmonic gap structure (*17*) and a supercurrent (*10*).

Neither subharmonic gap structures nor a supercurrent were observed experimentally, and so we can reasonably consider our devices at 4.2 K to consist of two independent interfaces in series. Within this picture, the crossover from the Andreev regime (V_g

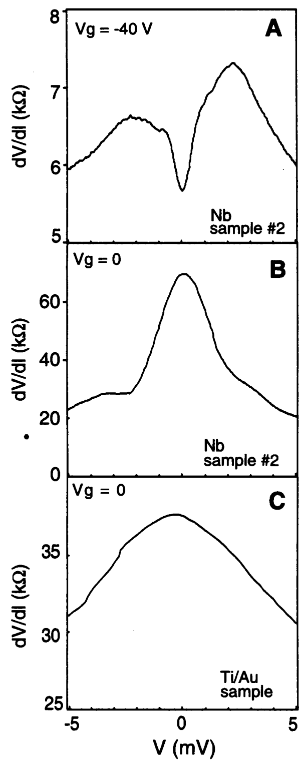

Fig. 3. (**A** and **B**) Differential resistance *dV/dI* versus bias voltage *V* for a sample with Nb electrodes at (A) $V_g = -40$ V and (B) $V_g = 0$ V. (**C**) For comparison, the differential resistance of a sample with normal metal electrodes (Ti-Au), over the same range of bias voltage (T = 4.2 K). Note that (A) and (B), respectively, show a dip and a peak at bias voltages below 2 to 3 mV, not seen in (C). The expected range of bias voltages for these features is ~2.9 mV, twice the gap of Nb (the factor of 2 accounting for two Nb-SWNT interfaces in series). Over this range of bias voltages, the relative size of the peak in *dV/dI* in the normal sample (C), one-tenth of the total resistance, is about 3% of the relative peak size for the Nb sample (B).

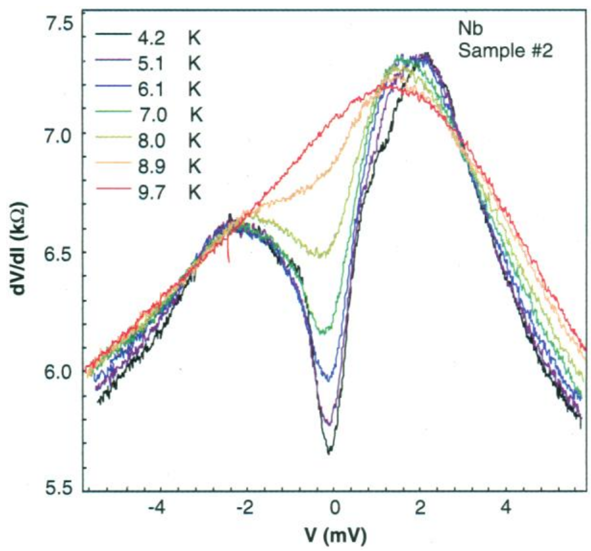

Fig. 4. Differential resistance *dV/dI* versus bias voltage *V* for a sample with Nb electrodes over a range of temperatures around T_c of Nb (9.2 K). The magnitude of the Andreev dip decreases with increasing *T* and disappears above T_c.

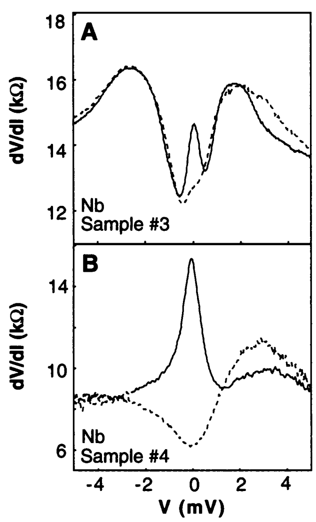

Fig. 5. (**A**) Differential resistance *dV/dI* versus bias voltage *V* for a sample with Nb electrodes measured at 4.2 K (dashed line) and 2 K (solid line), showing a narrow peak emerging from the center of the Andreev dip at lower temperatures (V_g = −40 V). (**B**) At a temperature of 40 mK, *dV/dI* may show either a peak or a dip, even at large negative gate voltage. This is different from what is found at 4.2 K, where *dV/dI* will always have a dip at sufficiently negative gate voltage. The low-temperature traces differ by only a few volts (dashed curve, V_g = −38 V; solid curve, V_g = −40 V) but show opposite curvatures around zero bias. The overall behavior at temperatures well below 4 K is not understood.

= −40 V) to the tunneling regime ($V_g = 0$ V) evident in Fig. 3 is a consequence of the changes in interface transparencies as a function of gate voltage. This conclusion is consistent with the expected properties of 0.3-μm ballistic (*13*) SWNTs, where changes in Fermi energy induced by typical gate voltages [for example, ~0.4 eV at $V_g = -40$ V (*12*)] are insufficient to alter the populations of electronic subbands. It is also in agreement with recent numerical results on how interface transparency depends on the Fermi energy in metallic nanotubes (*18*).

At temperatures down to 4.2 K, the qualitative picture in which either Andreev or tunneling processes dominate transport (*15*) works well. As the temperature is lowered further, new features appear that cannot be explained within this picture. Specifically, below ~4 K, a narrow peak in dV/dI emerges around zero bias, superimposed on the Andreev dip (Fig. 5A). This peak grows as the temperature is lowered, and by 40 mK dominates dV/dI measurements for almost all values of gate voltage, except for a few small intervals of V_g where a dip at zero bias can still be observed (Fig. 5B). No such peak is expected within a noninteracting picture. Similar low-temperature behavior of the differential resistance has been observed in two-dimensional electron gases connected to superconductors (*19, 20*), and has been tentatively attributed to electron-electron interactions (*21*). Electron-electron interaction may also explain the absence of subharmonic structure in dV/dI due to multiple Andreev reflections (*17*) as well as the absence of a supercurrent.

From this perspective, the recently reported observation by Kasumov *et al.* of a supercurrent in an individual SWNT sample as well as in SWNT ropes with superconducting contacts (*10*) is remarkable. It is particularly notable that the individual SWNT described in (*10*) had a higher normal-state resistance than in the present experiment [26 kilohms, compared to <18 kilohms (*22*)], which works against a proximity-induced supercurrent within a conventional picture. The experimental situation suggests that the basic physical mechanism responsible for a supercurrent in SWNT remains to be sorted out. The ability to control superconducting correlations in one dimension will greatly facilitate future study of this interesting phenomenon.

References and Notes

1. See D. Esteve, H. Pothier, S. Gueron, N. O. Birge, M. H. Devoret, in *Mesoscopic Electron Transport*, L. L. Sohn, L. P. Kouwenhoven, G. Schon, Eds. (Kluwer, Dordrecht, Netherlands, 1997), pp. 375–406; B. J. van Wees and H. Takayanagi, *ibid.*, pp. 469–501.
2. V. J. Emery, in *Highly Conducting One-Dimensional Solids*, J. T. Devresee, R. E. Evrard, V. E. van Doren, Eds. (Plenum, New York, 1979), pp. 247–303; J. Voit, *Rep. Prog. Phys.* **57**, 977 (1994).
3. S. Iijima, *Nature* **354**, 56 (1991); ______ and T. Ichihashi, *ibid.* **363**, 603 (1993).
4. S. J. Tans *et al.*, *ibid.* **386**, 474 (1997).
5. M. Bockrath *et al.*, *Science* **275**, 1922 (1997).
6. S. J. Tans, M. H. Devoret, R. J. A. Groenveld, C. Dekker, *Nature* **394**, 761 (1998).
7. D. H. Cobden, M. Bockrath, P. L. McEuen, A. G. Rinzler, R. E. Smalley, *Phys. Rev. Lett.* **81**, 681 (1998).
8. M. Bockrath *et al.*, *Nature* **397**, 598 (1999).
9. A. Bachtold *et al.*, *ibid.*, p. 673.
10. A. Yu. Kasumov *et al.*, *Science* **284**, 1508 (1999).
11. J. Kong, H. T. Soh, A. M. Cassell, C. F. Quate, H. Dai, *Nature* **395**, 878 (1998); T. H. Soh *et al.*, *Appl. Phys. Lett.* **75**, 627 (1999).
12. The capacitive coupling between the gate and the SWNTs can be estimated from the results of (*7*), which had a sample geometry essentially identical to ours. From those results, we infer that a change in gate voltage of 1 V corresponds to a change in Fermi energy of roughly 10 meV.
13. The present fabrication method yields low-resistance SWNTs over a broad range of tube lengths up to ~10 μm (A. F. Morpurgo *et al.*, unpublished data), with no apparent correlation between resistance and length. This suggests that electrons move ballistically in the tube, and that the measured resistance is dominated by the contacts.
14. M. Tinkham, *Introduction to Superconductivity* (McGraw-Hill, New York, ed. 2, 1996).
15. G. E. Blonder, M. Tinkham, T. M. Klapwijk, *Phys. Rev. B* **25**, 4515 (1982).
16. A. F. Andreev, *Zh. Eksp. Teor. Fiz.* **46**, 1823 (1964) [*Sov. Phys. JETP* **19**, 1228 (1964)].
17. M. Octavio, M. Tinkham, G. E. Blonder, T. M. Klapwijk, *Phys. Rev. B* **27**, 6739 (1983).
18. A. Rochefort, F. Lesage, D. R. Salahub, P. Avouris, preprint available at http://xxx.lanl.gov/abs/cond-mat/9904083. See the discussion on page 2.
19. See, for instance, figure 3A in H. Takayanagi and T. Akazaki, *Physica B* **249–251**, 462 (1998); J. P. Heida, thesis, University of Groningen (1998).
20. S. G. den Hartog, thesis, University of Groningen (1998).
21. See (*20*); for a possible theoretical explanation of the observations made on two-dimensional electron gases, see Y. Oreg, P. W. Brouwer, B. D. Simons, A. Altland, *Phys. Rev. Lett.* **82**, 1269 (1999).
22. For instance, in sample 2, three SWNTs in parallel gave a low-temperature resistance of 6 kilohms, implying that at least one of the three tubes is below 18 kilohms. Similar values below 20 kilohms can be inferred for the other samples as well.

23. We thank B. J. van Wees for useful discussions, and N. Iosad and D. Wilms Floet for high-quality Nb sputtering. Supported by the NSF Presidential Faculty Fellowship program (grant DMR-9629180-1), the NSF Partnership for Nanotechnology program (grant ECS-9871947), the Stanford Center for Materials Research (an NSF-Materials Research Science and Engineering Center), the National Nanofabrication Users Network (funded by NSF grant ECS-9731294), the Camile Henry-Dreyfus Foundation, and the American Chemical Society.

9 June 1999; accepted 31 August 1999

Evidence for One-Dimensional Charge Transport in $La_{2-x-y}Nd_ySr_xCuO_4$

Takuya Noda, Hiroshi Eisaki, Shin-ichi Uchida

Doping dependences of the resistivity and the Hall coefficient are presented for neodymium-doped lanthanum strontium cuprate ($La_{1.4-x}Nd_{0.6}Sr_xCuO_4$) in the static spin-charge stripe ordered phase. For doping concentration $x \leq 1/8$, a rapid decrease in the magnitude of the Hall coefficient at low temperatures provides evidence for one-dimensional charge transport, whereas for $x > 1/8$, the Hall coefficient remains relatively large in the ordered phase. The results indicate a crossover from one- to two-dimensional charge transport taking place at $x = 1/8$.

The one-dimensional (1D) spin-charge density modulations in the two-dimensional (2D) CuO_2 planes, or stripe phase, was proposed by Tranquada *et al.* (*1*) to account for the anomalous behavior in $La_{2-x-y}Nd_ySr_xCuO_4$ (*2*), in which slight changes in the crystal structure lead to suppression of the superconductivity. Elastic neutron scattering experiments on $La_{2-x-y}Nd_ySr_xCuO_4$ (LNSCO) with x near the "magic number"—1/8—have demonstrated that the compound exhibits spin-charge order with the periodicity eight and four times that of the lattice unit cell, respectively (*1*). Similar spin-charge orders have been observed for other values of x (*3*), where the periodicity of the static spin correlation has almost the same x dependence as that observed in the incommensurate inelastic neutron scattering peaks in $La_{2-x}Sr_xCuO_4$ (LSCO) (*4*), suggesting that spin-charge modulations exist in superconducting LSCO. Furthermore, recent neutron-scattering experiments on $YBa_2Cu_3O_{7-y}$ (*5*) and $Bi_2Sr_2CaCu_2O_8$ (*6*) suggest that the stripe fluctuations may be inherent to the doped CuO_2 planes. The possibility of the formation of stripes had been discussed before these new findings (*7*) and it is proposed that the dynamic stripe fluctuation is a possible driving force for high-temperature superconductivity (HTSC) (*8*).

However, in spite of the accumulated interest, because of a lack of direct evidence for one-dimensionality, full consensus on the existence of spin-charge stripes has not been established. The difficulty is that the spin-charge stripes in the adjacent CuO_2 plane are directed by 90° to each other, as suggested from the neutron and x-ray scattering measurements (*1,*

Department of Superconductivity, The University of Tokyo, Tokyo 113-8656, Japan.

LINKED CITATIONS

You have printed the following article:

Gate-Controlled Superconducting Proximity Effect in Carbon Nanotubes
A. F. Morpurgo; J. Kong; C. M. Marcus; H. Dai
Science, New Series, Vol. 286, No. 5438. (Oct. 8, 1999), pp. 263-265.
Stable URL:
http://links.jstor.org/sici?sici=0036-8075%2819991008%293%3A286%3A5438%3C263%3AGSPEIC%3E2.0.CO%3B2-S

This article references the following linked citations:

References and Notes

[5] **Single-Electron Transport in Ropes of Carbon Nanotubes**
Marc Bockrath; David H. Cobden; Paul L. McEuen; Nasreen G. Chopra; A. Zettl; Andreas Thess; R. E. Smalley
Science, New Series, Vol. 275, No. 5308. (Mar. 28, 1997), pp. 1922-1925.
Stable URL:
http://links.jstor.org/sici?sici=0036-8075%2819970328%293%3A275%3A5308%3C1922%3ASTIROC%3E2.0.CO%3B2-5

[10] **Supercurrents Through Single-Walled Carbon Nanotubes**
A. Yu. Kasumov; R. Deblock; M. Kociak; B. Reulet; H. Bouchiat; I. I. Khodos; Yu. B. Gorbatov; V. T. Volkov; C. Journet; M. Burghard
Science, New Series, Vol. 284, No. 5419. (May 28, 1999), pp. 1508-1511.
Stable URL:
http://links.jstor.org/sici?sici=0036-8075%2819990528%293%3A284%3A5419%3C1508%3ASTSCN%3E2.0.CO%3B2-L

NOTE: *The reference numbering from the original has been maintained in this citation list.*